JOURNAL OF GUIDANCE, CONTROL, AND DYNAMICS
Vol. 18, No. 2, March–April 1995

Dual-Mode Disturbance-Accommodating Pointing Controller for Hubble Space Telescope

Stewart I. Addington*
Teledyne Brown Engineering, Huntsville, Alabama 35807
and
C. D. Johnson†
University of Alabama in Huntsville, Huntsville, Alabama 35899

Cyclic thermal expansions and mechanical stiction effects in the solar arrays on the Hubble Space Telescope (HST) are triggering repeated occurrences of damped, relaxation-type flex-body vibrations of the solar arrays. Those solar array vibrations are, in turn, causing unwanted deviations of the telescope from its specified pointing direction. In this paper we propose two strategies one can adopt in designing a telescope-pointing controller to cope with the aforementioned disturbances: 1) a *total isolation* (TI) control strategy whereby the HST controller torques are designed to adaptively counteract and cancel out the persistent disturbing torques that are causing the unwanted telescope motions and 2) an *array damping* (AD) control strategy whereby the HST controller torques are used to actively augment the natural dampening of the solar array vibrations and the attendant telescope motions, between triggerings of the stiction-related flex-body relaxation oscillations. Using the principles of disturbance accommodation control theory, a dual-mode controller for a generic, planar-motion (single-axis) model of the HST is proposed. This controller incorporates both the TI and AD modes of disturbance accommodation. Simulation studies of the closed-loop system using generic parameter values clearly indicate, qualitatively, the enhanced pointing performance such a controller can achieve.

Introduction

THE two large deployable solar array panels attached in a cantilever-beam fashion to opposite sides of the Hubble Space Telescope (HST) main body (Fig. 1) have introduced a new dimension to the problem of controlling the HST's pointing direction. In particular, the uneven thermal expansions of the solar array's collapsible structural members, caused by cyclic solar heating effects, and mechanical coulomb friction/stiction effects that resist thermal expansions between structural members are causing persistent, jerky, "flapping" motions of those solar arrays. Those flex-body flapping motions are of a damped-oscillation type and are triggered in a sporadic, random like manner, depending on the intensity of the solar heating/cooling and on the stiction thresholds associated with sliding interactions between various structural members of the arrays.

Those flapping motions of the solar arrays induce, through their attachment points with the main body of the HST, a series of randomly triggered damped-oscillation disturbance torques that cause the HST main body to veer away from the precision point needed to satisfy experiment requirements. Thus, an effective HST pointing control system must cope with this uncertain disturbance environment.

In this paper we will derive a new conceptual form of HST controller that effectively accomplishes this goal. Simulation results using a nonlinear, planar motion model of the HST with generic parameter values demonstrate the effectiveness of the proposed new controller in a single-axis control context. A generalization of the control concepts presented here, to include full three-axis control of the HST, should provide a significant enhancement to the actual HST pointing performance.

Due to space limitations imposed on the present paper, some of the detailed derivations and calculations could not be included here. However, those details are contained in various appendices of Ref. 1 and those sources are cited herein, wherever relevant.

Received Oct. 15, 1993; revision received March 15, 1994; accepted for publication Sept. 23, 1994.

*Astrodynamics Engineer.

†Professor, Department of Electrical and Computer Engineering.

Characterization of Solar Array Flapping Disturbances in HST Control Problem

The randomly triggered flapping solar arrays pose a unique challenge to the HST control system design because the uncertain disturbance torques they induce to the HST main body are not effectively modeled as steady-state random processes with known means and variances. Consequently, traditional stochastic control theories[2] are ineffective in accomplishing high-performance precision pointing of the HST in the face of those flapping solar arrays.

The essential feature of the HST uncertain disturbance torques due to flapping solar arrays is that, once triggered, they have a distinguishable damped-oscillation type waveform characteristic that may have varying initial conditions but is always relatively smooth and well behaved (compared to the virtually continuous fusillade of triggering events associated with mathematical white noise). Thus, for instance, individual components (modes) $w_i(t)$ of the HST uncertain disturbance torques due to the solar arrays can be rather accurately represented (modeled) by a mathematical spline expression of the form

$$w_i(t) = C_1 e^{-\beta_i t} \sin \omega_i t + C_2 e^{-\beta_i t} \cos \omega_i t \tag{1}$$

where $\beta_i > 0$ denotes the damping parameter and $\omega_i > 0$ denotes the oscillation frequency and where the spline weighting constants C_1, C_2 in Eq. (1) are allowed to jump in value from time to time, in an uncertain, randomlike manner [thereby allowing for different initial conditions on Eq. (1) at each triggering event]. The numerical values of (β_i, ω_i) in Eq. (1) can be estimated from examination of actual flight data, results of ground experiments, etc.

It can be argued that, in practice, the parameters β_i, ω_i in Eq. (1) might be subject to some degree of uncertain, time-dependent variation due to wear, distortions, thermal effects, etc., which may render the model (1) ineffective. In such cases, an effective alternative to Eq. (1) is the considerably more robust polynomial-spline representation

$$w_i(t) = C_1 + C_2 t + C_3 t^2 + \cdots + C_m t^{(m-1)} \tag{2}$$

where m is an appropriate positive integer and, as in Eq. (1), the weighting constants $C_1, C_2, \ldots, C_m$ are allowed to jump in value

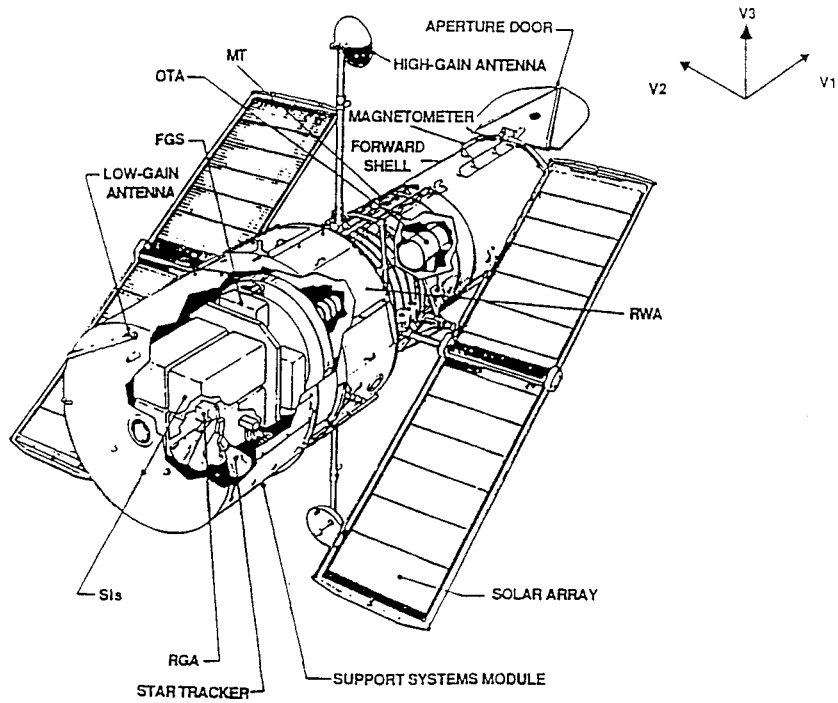

Fig. 1 HST with deployed solar arrays.

in an uncertain, once-in-a-while fashion, hereafter called stepwise-constant behavior. Expression (2) can effectively represent a broad class of uncertain, meandering-type functions $w_i(t)$, including complex "oscillations" of the type (1) with completely unknown waveform characteristics. In practice, satisfactory results using Eq. (2) can usually be achieved even with relatively small values for m, typically $m = 3, 4$ (the so-called quadratic and cubic spline models, respectively).

In summary, individual modes of the uncertain disturbance torques associated with flapping solar arrays on the HST have relatively smooth, well-behaved, time-domain waveform characteristics of the randomly triggered, damped-oscillation type. Consequently, those disturbance torques are effectively represented by mathematical spline expressions of the form (1) or (2). It is remarked that, in some situations, a combination of Eqs. (1) and (2) may be most effective in representing an uncertain flex-body vibration mode.

Accommodation of Solar Array Disturbances in HST

As stated earlier, the HST disturbance torques associated with flapping solar arrays cause the point of the HST main body to deviate from the desired direction. Thus, it is clear that those persistent disturbances cause only unwanted, upsetting effects. Consequently, the primary goal of the HST controller, with respect to accommodating those disturbances, should be to (ideally) generate opposing control torques that automatically adapt to and cancel out (counteract) the persistent disturbance torques and their upsetting effects in real time. Under this latter mode of control, the main body of the HST would be effectively isolated from the disturbing motions of the flapping solar arrays, so that the point of the HST could be regulated as if there were no solar array flapping motions. Hence, we hereafter refer to this as the total isolation (TI) mode of control.

In the TI mode of control, no effort is made to mitigate the flapping motions of the solar arrays themselves. However, the (mild) natural structural damping effects in the solar array structures will tend to dampen out those oscillations until such time that the oscillations are once again triggered by another thermal/stiction relaxation effect. In some situations, it may be desirable to employ the HST controller to hasten the natural damping-out of the solar array oscillations. This can be accomplished by designing the HST controller to create strategic rocking motions of the HST main body that are so timed and phased as to accomplish active damping (damping augmentation) of the solar array oscillations. We hereafter call this the array damping (AD) mode of control. Practical realization of the AD mode of control would seem to require a relatively "smart" type of HST controller. However, it will be shown that a simple linear controller will do the job.

The TI and AD modes of control constitute what we believe to be the two main options to be considered in designing the HST controller to accommodate uncertain oscillations of the solar arrays. For maximum flexibility in implementations, it is desirable to have a mode-switching arrangement for the TI/AD control laws, whereby one can gracefully shift control action from the TI mode to the AD mode (and vice-versa) in real time, as dictated by the real-time needs on-station.

In subsequent sections of this paper we will demonstrate how a unique branch of modern control [disturbance accommodation control (DAC) theory][3–7] enables one to systematically design physically realizable, all-linear, time-invariant controllers that embody the TI and AD modes of disturbance accommodation described in this section.

Simplified, Planar-Motion Configuration Model of HST

The objective of this paper is to develop and demonstrate the performance characteristics of a new control concept for the HST pointing controller design. For this purpose, we will consider a simplified planar-motion (single-axis) generic configuration model of the HST (Fig. 2) in which the inertias and flex-body (flapping) motions of the attached solar arrays are represented by rigid, movable arms attached to either side of the HST main body through idealized "pin-joints." To replicate one mode of the structural flexibility and structural damping effects of each of the solar arrays, the back-and-forth oscillations $\theta_1(t)$, $\theta_2(t)$ of the two arms about their respective pin-joints are considered to be resisted by linear torsional "spring" and linear viscous "damping" effects that may be different for each arm. The normal (equilibrium) positions of the arms are perpendicular to the HST main body.

To simultaneously replicate multiple flex-body modes of the solar arrays, one simply imagines multiple rigid arms attached to each of the two pin-joints in Fig. 2, where the rotational spring constant, damping, mass, and inertia of each arm is chosen to conform to the known frequency, damping, and inertial properties of the particular flex-body mode being replicated. In this way one can consider as many simultaneous flex-body solar array modes (and flex-body modes of other HST appendages) as desired using the pin-jointed

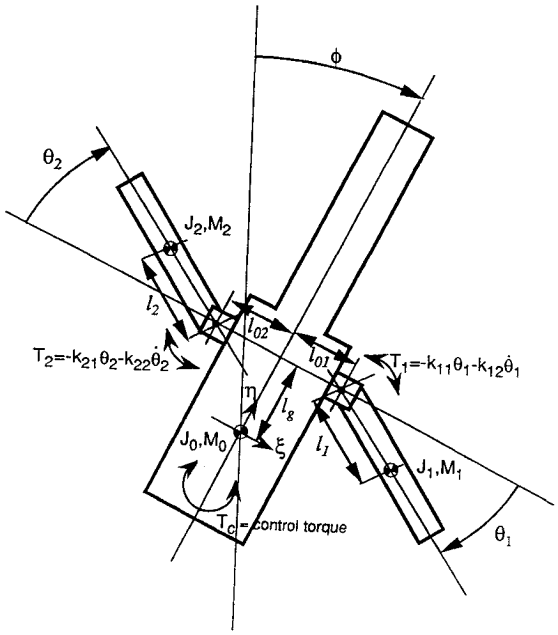

Fig. 2 Planar-motion (single-axis) configurational model of HST and attached solar arrays (replicating one flex-body mode for each solar array).

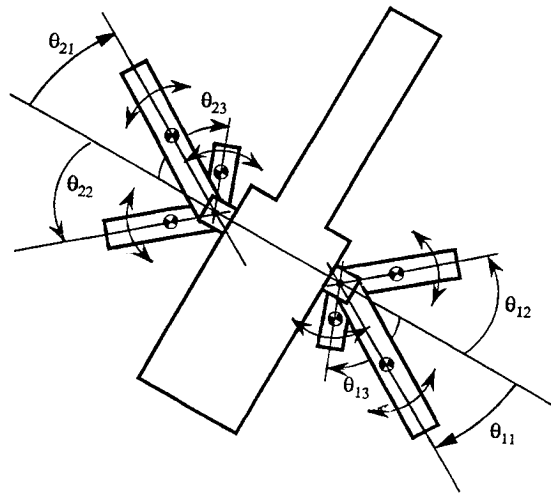

Fig. 3 Planar-motion (single-axis) configuration model of HST and attached solar arrays (replicating three flex-body modes for each solar array).

rigid-arm technique as shown in Fig. 3. Our decision to consider here only one flex-body mode (Fig. 2) for each solar array is motivated by the concept demonstration nature of this paper. In particular, we wish to avoid introducing additional complexity that is not essential to illustrating the basic concepts of our HST modeling and control design procedure.

The planar-motion, concept demonstration model in Fig. 2 can be viewed as representing the actual HST when the solar arrays are rotated such that the flapping motions of each solar array consist of essentially one flex-body mode (which may be different for each array) and such that the associated disturbance torques induced to the HST main body cause relatively little out-of-plane rotational motions of the main body. The new controller scheme we develop here for the single-axis model in Fig. 2 can be employed in each of the other two (rotational) axes (with proper coordination imposed between each such controller) to achieve full three-axis coordinated control of the HST main-body rotations for arbitrary positioning of the solar array panels.

It is remarked that our introduction of the simplified, planar-motion HST configuration model in Fig. 2 was not motivated by a desire to keep things simple, but rather by the technological necessity of having a mathematical model of the HST that is based on "first principles" of dynamics. In particular, the ability to derive a controller that accomplishes the TI mode of disturbance accommodation, as described in the previous section, requires that one begin with an HST mathematical model that embodies the actual dynamic equations of motion for the HST main body and for the interface dynamics associated with each of the attached solar arrays. Alternative mathematical models based on modal decompositions and/or transfer function methodologies might not provide such detailed information and may "obscure" some novel control possibilities such as the TI mode of control we develop here.

Exact Equations of Motion for Planar-Motion HST Model in Fig. 2

The simplified, planar-motion HST configuration model in Fig. 2 is, in fact, rather "complicated" from the dynamics point of view. In fact, the derivation of the exact equations of motion for Fig. 2 would be extremely difficult and time consuming using any of the classical methods of dynamics, such as Newton's, Lagrange's, or Hamilton's methods. For this study, the exact equations of motion for Fig. 2 were derived, in completely general, explicit, symbolic form, using the method of Kane's equations[8] as implemented in the computer-aided modeling program AUTOLEV. The resulting mathematical model consists of a set of five simultaneous, second-order, highly nonlinear differential equations that can be written in the vector-matrix form

$$\boldsymbol{M}(y)\ddot{y} + \boldsymbol{D}\dot{y} + \boldsymbol{K}y + f(y, \dot{y}) = \boldsymbol{b}u \tag{3}$$

where y is the 5-vector of position variables $y = (\phi, \theta_1, \theta_2, \xi, \eta)$ as defined in Fig. 2 and u is the (single-axis) HST main-body control torque relevant to the planar-motion configuration shown in Fig. 2. The elements of the 5×5 matrices $\{\boldsymbol{M}, \boldsymbol{D}, \boldsymbol{K}\}$ and of the vectors $\{\boldsymbol{b}, f(y, \dot{y})\}$ in Eq. (3) are determined by various masses, inertias, lengths, etc., and their explicit expressions are given in Appendix A of Ref. 1. Those expressions are completely general in the sense that they are given in terms of arbitrary, symbolic masses, inertias, lengths, etc.

The natural dynamic behavior of the mathematical model (3) turns out to be surprisingly complicated, rich in diversity, and often counterintuitive, owing to the strong, nonlinear *inertia coupling* that exists between the motions $\{\phi(t), \theta_1(t), \theta_2(t), \xi(t), \eta(t)\}$. That inertia coupling effect is manifested in the highly *nonsparse* structure of the nonconstant *mass-matrix* $\boldsymbol{M}(y)$ in Eq. (3) that has the form [it turns out that $m_{ij} = m_{ij}(\theta_1, \theta_2)$, in general; see Appendix A of Ref. 1 for explicit m_{ij} expressions]

$$\boldsymbol{M} = \begin{bmatrix} m_{11} & m_{12} & m_{13} & m_{14} & m_{15} \\ m_{21} & m_{22} & 0 & m_{24} & m_{25} \\ m_{31} & 0 & m_{33} & m_{34} & m_{35} \\ m_{41} & m_{42} & m_{43} & m_{44} & 0 \\ m_{51} & m_{52} & m_{53} & 0 & m_{55} \end{bmatrix} \tag{4}$$

We will now proceed to show how one can develop TI and AD controllers for the HST model in Fig. 2 using the exact equations of motion (3) and (4).

HST Controller Designs for Total Isolation and Array-Damping Modes of Control

In this section we will use the general, symbolic-based equations of motion (3) and (4) to develop corresponding general, explicit symbolic expressions for HST controllers that achieve the TI and AD modes of control. For this purpose, we will consistently assume the only available output measurement is $\phi(t)$. If additional measurements [say $\dot{\phi}(t)$] are available, the structure of the state observers (Kalman filters) used herein can be modified accordingly; see Appendix C of Ref. 1. In addition, we will disregard the control actuator limitations to permit better appreciation for the ultimate performance capabilities of the proposed controllers.

Design of Total Isolation Controller

The primary task of the HST controller is to regulate the point $\phi(t)$ of the HST main body to a specified setpoint ϕ_{sp} and accurately maintain $\phi(t) \approx \phi_{sp}$ for a specified time period. It is recalled that in the TI mode of control this task is accomplished, in the face of uncertain, unmeasurable disturbance torques created by the "flapping" solar arrays, by generating time-varying HST controller torques that automatically adapt to and synchronize with the time-varying disturbance torques (in an equal-but-opposite manner) and thereby cancel out their disruptive effects on $\phi(t)$ in real time. We will now show how to design such a controller using the principles of DAC theory.[3-7] For simplicity, it will hereafter be assumed that $\phi_{sp} = 0$. Nonzero values of ϕ_{sp} can be accommodated by well-known, simple modifications of the results presented here.

Design of the TI mode of control begins by identifying the particular second-order equation of motion that governs the HST main-body rotation $\phi(t)$ in Fig. 2. That equation can be obtained by first multiplying Eq. (3) by $\boldsymbol{M}^{-1}(y)$ to obtain (the existence of $\boldsymbol{M}^{-1}$ is established in Appendix B of Ref. 1)

$$\ddot{y} + \boldsymbol{M}^{-1}(y)\boldsymbol{D}\dot{y} + \boldsymbol{M}^{-1}(y)\boldsymbol{K}y + \boldsymbol{M}^{-1}(y)f(y, \dot{y}) = \boldsymbol{M}^{-1}(y)\boldsymbol{b}u \quad (5)$$

and then reading off the first of the five equations represented by Eq. (5). The result is the second-order, nonlinear equation of motion

$$\ddot{\phi} + g(\theta_1, \theta_2, \dot{\theta}_1, \dot{\theta}_2, \dot{\phi}, \dot{\xi}, \dot{\eta}) = h(\theta_1, \theta_2)u \quad (6)$$

where the precise expressions for the functions $g(\cdot)$, $h(\cdot)$ are given in (C.2) and (C.3) of Appendix C of Ref. 1. Expression (6) governs the actual angular motions $\phi(t)$ of the HST main body, as shown in Fig. 2, for an arbitrary control torque input $u(t)$. Note that the one term $g(\cdot, \cdot, \cdot)$ in Eq. (6) embodies all of the disturbing torques induced on the HST main body by the flapping motions of the solar arrays in Fig. 2.

At this point, it is useful to introduce the notion of an ideal model for the desired controlled (closed-loop) motions $\phi(t)$ in the TI mode of control. For this purpose, we assume the desired behavior of $\phi(t)$ in the TI mode is represented by the solutions of the specified (given) ideal-model differential equation

$$\ddot{\phi} + (2\zeta\omega_n)\dot{\phi} + (\omega_n^2)\phi = 0 \quad (7)$$

where the values of the parameters ($\zeta > 0$, $\omega_n > 0$) are assumed specified. Thus, the control designer's task is to design the control function $u = u(?)$ in Eq. (6) to make this equation "look like" Eq. (7). In the idealistic case, where all arguments in $g(\cdot)$, $h(\cdot)$ can be accurately measured in real time, it is clear that the ideal choice for the TI controller $u(\cdot)$ in Eq. (6) would be

$$u = h^{-1}(\theta_1, \theta_2)[-k_2\dot{\phi} - k_1\phi + g(\theta_1, \theta_2, \dot{\theta}_1, \dot{\theta}_2, \dot{\phi}, \dot{\xi}, \dot{\eta})] \quad (8)$$

where

$$k_1 = \omega_n^2, \qquad k_2 = 2\zeta\omega_n \quad (9)$$

However, for this study it is assumed that only $\phi(t)$ can be measured in real time. Thus we will seek a physically realizable approximation to Eq. (8) as follows. First, the term $h(\theta_1, \theta_2)$ in Eq. (6) will be approximated by a fixed constant $\hat{h}$ that is selected to approximate the range of values $h(\theta_1, \theta_2)$ for a representative range of (θ_1, θ_2) values. (The determination of $\hat{h}$ is presented in Appendix B of Ref. 1.) Next, the function $g(\cdot, \cdot, \cdot)$ in Eq. (8) will be viewed and treated as an unknown, time-varying "disturbance" term $g(t)$ defined by

$$g(t) = g(\theta_1(t), \theta_2(t), \dot{\theta}_1(t), \dot{\theta}_2(t), \dot{\phi}(t), \dot{\xi}(t), \dot{\eta}(t)) \quad (10)$$

where $\{\theta_1(t), \theta_2(t), \phi(t), \xi(t), \eta(t)\}$ are arbitrary solutions of the exact equations of motion (3). A typical time plot of Eq. (10) is shown in Fig. 4, where it can be seen that the unknown disturbance $g(t)$ is a smooth, well-behaved function that slowly meanders back and forth in an oscillating manner. We will now show how one can estimate the time function $g(t)$ in real time from real-time measurements of $\phi(t)$. Thus, following the principles of DAC theory (Ref. 4, p. 412), we first represent the uncertain time behavior of $g(t)$ by a quadratic polynomial spline [see Eq. (2)]:

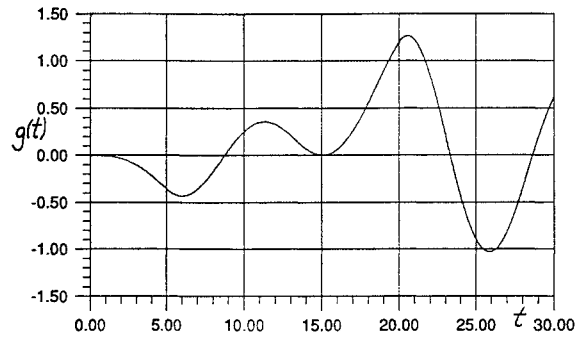

Fig. 4 Typical time-plot of $g(t)$ in Eq. (10).

$$g(t) = C_1 + C_2 t + C_3 t^2 \quad (11)$$

where the weighting "constants" C_i in Eq. (11) are allowed to jump in a once-in-a-while, stepwise-constant manner, as described below Eq. (2). Next we introduce a state-variable model for $g(t)$ by defining

$$z_1 = g(t), \qquad z_2 = \dot{g}(t), \qquad z_3 = \ddot{g}(t) \quad (12)$$

and observing that the z_i obey the differential equations

$$\dot{z}_1 = z_2 + \sigma_1(t), \qquad \dot{z}_2 = z_3 + \sigma_2(t), \qquad \dot{z}_3 = \sigma_3(t) \quad (13)$$

where the symbols $\sigma_i(t)$ in Eq. (13) denote totally unknown, unmeasurable, sparsely populated time sequences of randomly arriving, random-intensity impulses (Dirac impulses). Those impulses represent the "cause" of the once-in-a-while jumping of the C_i values in Eq. (11).

The foregoing arguments and approximations enable us to rewrite the exact equation of motion (6) for $\phi(t)$ in the approximate and simplified form

$$\ddot{\phi} = \hat{h}u - w(t), \qquad \hat{h} \approx h, \qquad w(t) = g(t) \quad (14)$$

where, according to Eq. (12), the disturbance term $w(t)$ in Eq. (14) is given by

$$w(t) = z_1(t) \quad (15)$$

and where $z_1(t)$ is (approximately) governed by the set of impulse-forced differential equations (13). The TI control law (8) corresponding to Eq. (14) thus becomes the constant-gain linear control law

$$u = \hat{h}^{-1}[-k_2\hat{\dot{\phi}} - k_1\phi + \hat{z}_1(t)] \quad (16)$$

where k_1, k_2 are defined as in Eq. (9), and where, following standard DAC techniques (Ref. 4, p. 430), $\hat{\dot{\phi}}(t)$ and $\hat{z}_1(t)$ denote on-line, real-time estimates of $\dot{\phi}(t)$ and $z_1(t)$ obtained from a composite plant/disturbance state observer (Kalman filter) based on the approximate plant model (14) and the disturbance model (13). That composite state observer operates on the plant output measurement $\phi(t)$ and plant control input $u(t)$ to produce accurate real-time estimates of the state variables $\{x_1 = \phi, x_2 = \dot{\phi}\}$ for the *actual* plant (6) as well as estimates of the state variables $\{z_1 = g(t), z_2 = \dot{g}(t), z_3 = \ddot{g}(t)\}$ for the disturbance term $w(t)$ in Eq. (14). The design of the composite state observer for this TI mode of control is described in Appendix C of Ref. 1.

Substituting the control expressions (16) and (9) in the *actual* equation of motion (6) yields the actual closed-loop equation of motion for $\phi(t)$ in the TI mode as

$$\ddot{\phi} + g(\cdot, \cdot, \cdot) = h(\cdot, \cdot)\hat{h}^{-1}[-k_2\hat{\dot{\phi}} - k_1\phi + \hat{z}_1(t)] \quad (17)$$

which can be rearranged to read

$$\ddot{\phi} + h\hat{h}^{-1}[(2\zeta\omega_n)\hat{\dot{\phi}} + (\omega_n^2)\phi] = -g(\cdot, \cdot, \cdot) + h\hat{h}^{-1}[\hat{z}_1(t)] \quad (18)$$

Comparison of Eq. (18) with Eq. (7) shows that the desired ideal-model behavior of $\phi(t)$ in the TI mode of control will be realized, provided the assumed approximations

$$\hat{h}(\cdot,\cdot)\hat{h}^{-1} \approx 1, \qquad \hat{\dot{\phi}} \approx \dot{\phi}(t)$$

$$\hat{z}_1(t) \approx g(\theta_1(t), \theta_2(t), \dot{\theta}_1(t), \dot{\theta}_2(t), \dot{\phi}(t), \dot{\xi}(t), \dot{\eta}(t)) \quad (19)$$

are achieved by the aforementioned design procedure. This completes the design of the HST controller for the TI mode of control.

Design of AD Controller

The TI mode of control automatically isolates the HST main body from any disturbance torques induced by the flapping solar arrays and is therefore proposed as the normal control mode for HST pointing experiments. On the other hand, one can imagine exceptional situations in which the prompt damping of excessive solar array oscillations becomes a primary concern. For those situations, the optional AD mode of control provides a means for actively augmenting the natural damping of the solar array oscillations by carefully controlled and orchestrated dynamic motions of the HST main body. To achieve this active augmentation to the solar arrays' natural structural effects, the AD controller must maneuver the HST main-body motions $\phi(t)$ back and forth, so as to induce controlled, time-varying, "bending torques" [at the body/solar array attachment point (structural interface)] that are strategically timed to dissipate the energy of the oscillating solar arrays themselves. It is rather surprising that this seemingly complex, intricate control task can be accomplished by a simple, constant-gain, linear controller, as we shall now show.

The design of the AD mode of control begins by identifying the particular subset of the complete equations of motion (3) that governs the motions $\phi(t), \theta_1(t), \theta_2(t)$. That particular subset consists of the first three second-order differential equations (5), which can be separated out from Eq. (3) and written as

$$\ddot{\bar{y}} + \bar{\boldsymbol{D}}(\bar{y})\dot{\bar{y}} + \bar{\boldsymbol{K}}(\bar{y})\bar{y} + \bar{f}(y, \dot{y}) = \bar{\boldsymbol{b}}(\bar{y})u \quad (20)$$

where $\bar{y} = (\phi, \theta_1, \theta_2)$ and $\bar{\boldsymbol{D}}(\bar{y})$, $\bar{\boldsymbol{K}}(\bar{y})$, $\bar{f}(y, \dot{y})$, $\bar{\boldsymbol{b}}(\bar{y})$ can be determined from $\boldsymbol{M}^{-1}\boldsymbol{D}$, $\boldsymbol{M}^{-1}\boldsymbol{K}$, etc., in Eq. (6). Next, one must linearize Eq. (20) in the neighborhood of the anticipated operating-point values of $\{\phi(t), \theta_1(t), \theta_2(t)\}$. For our problem those operating-point values are

$$\phi = \dot{\phi} = 0, \qquad \theta_1 = \dot{\theta}_1 = 0, \qquad \theta_2 = \dot{\theta}_2 = 0 \quad (21)$$

Linearizing Eq. (20) in the neighborhood of Eq. (21) using standard procedures then yields Eq. (20) in the linear, constant-coefficient form (note: $\bar{f}(y, \dot{y}) = 0$ at $\phi = \dot{\phi} = \theta_1 = \dot{\theta}_1 = \theta_2 = \dot{\theta}_2 = 0$)

$$\ddot{\bar{y}} + \tilde{\boldsymbol{D}}\dot{\bar{y}} + \tilde{\boldsymbol{K}}\bar{y} = \tilde{\boldsymbol{b}}u \quad (22)$$

where $\{\tilde{\boldsymbol{D}}, \tilde{\boldsymbol{K}}, \tilde{\boldsymbol{b}}\}$ denote the values of $\{\bar{\boldsymbol{D}}(\bar{y}), \bar{\boldsymbol{K}}(\bar{y}), \bar{\boldsymbol{b}}(\bar{y})\}$ at the operating values (21). In the AD control mode the objective is to simultaneously achieve the three stabilization conditions

$$\phi(t) \to 0, \qquad \theta_1(t) \to 0, \qquad \theta_2(t) \to 0 \quad (23)$$

For this purpose we first seek $u(\cdot)$ in the (idealistic) constant-gain linear state feedback form

$$u = k_c^{\mathrm{T}} \begin{bmatrix} \bar{y} \\ \dot{\bar{y}} \end{bmatrix} = k_{c1}\phi + k_{c2}\theta_1 + k_{c3}\theta_2 + k_{c4}\dot{\phi} + k_{c5}\dot{\theta}_1 + k_{c6}\dot{\theta}_2 \quad (24)$$

where the six elements of the control gain vector $k_c = (k_{c1}, \ldots, k_{c6})$ are chosen to place the corresponding six (closed-loop) eigenvalues $\{\lambda_1, \ldots, \lambda_6\}$ of Eq. (22) at suitable "stable" locations in the complex plane. An effective procedure for computing the gains $\{k_{c1}, \ldots, k_{c6}\}$ is outlined in Appendix C of Ref. 1. For our simulation studies, we selected the six λ_i to consist of three identical pairs of stable, complex-conjugate roots defined by

$$\lambda = -\zeta\omega_n \pm j\omega_n\sqrt{1-\zeta^2}, \qquad j = \sqrt{-1} \quad (25)$$

where $\zeta > 0, \omega_n > 0$ are chosen to yield satisfactory closed-loop response characteristics for the AD mode.

The final step in the design of the AD control mode is to develop a state observer (Kalman filter) that generates accurate real-time estimates of $\dot{\phi}(t), \theta_1(t), \dot{\theta}_1(t), \theta_2(t), \dot{\theta}_2(t)$ from the available measurement $\phi(t)$, as needed to implement the AD control law (24). For this purpose we developed a conventional full-order observer based on the linearized model (22). The details of that observer design are presented in Appendix C of Ref. 1. The outputs $\hat{\dot{\phi}}(t), \hat{\theta}_1(t), \hat{\dot{\theta}}_1(t), \hat{\theta}_2(t), \hat{\dot{\theta}}_2(t)$ of that observer are used in place of their idealized counterparts in Eq. (24) for implementation of the AD control mode. This completes the design of the HST controller for the AD mode of control.

Summary of Proposed Dual-Mode Disturbance-Accommodating Controller for HST

The new HST controller proposed in this study for the single-axis model in Fig. 2 consists of two distinct controller algorithm configurations, one for the TI mode of control and one for the AD mode of control. The TI controller is given by Eq. (16) and its associated state observer [Ref. 1, Appendix C, (C.14)], where the parameters ζ, ω_n are assumed chosen to yield the desired quality of closed-loop regulation response $\phi(t) \to 0$. The AD controller is given by Eq. (24) and its associated state obsever [Ref. 1, Appendix C, (C.27)], where the design parameters ζ, ω_n can be chosen to yield the desired "settling time" for the actively augmented damping of the solar array oscillations.

In both the TI and AD modes of control, the presumed real-time plant output measurements for the planar-motion configuration of Fig. 2 consist of the HST main-body pointing angle $\phi(t)$ *only*. If it should turn out that one can also accurately measure the rate $\dot{\phi}(t)$ in real time, that additional measurement can be incorporated into the composite plant state/disturbance state observers associated with Eqs. (16) and (24); see Appendix C of Ref. 1.

In any consideration of a dual-mode controller, the question of how to gracefully "switch" from one mode to the other naturally arises. In principle, such mode switchings are usually accomplished by a slow "fading" from one mode to another, similar to the way one fades signals from right to left speakers in a stereo sound system. However, this fading procedure must be done in such a way that one control mode does not tend to "fight" the other control mode during the fading/mixing process. In this study it was found necessary to fade one control mode to zero before fading on the other control mode to avoid the fighting effect.

Generic Parameter Values for Simulation Exercises of Closed-Loop Planar-Motion HST Model (Fig. 2)

The numerical parameter values provided for the mathematical models supplied by NASA for this project were not appropriate for the alternative first-principles, planar-motion dynamic model (3) we derived for our controller design procedure. Consequently, for our closed-loop simulation studies of the HST model in Fig. 2, we chose a set of numerical parameter values [for the various masses, inertias, lengths, etc., indicated in Fig. 2 and in the analytical model (3)] that seem to be representative of the relative scale of values associated with the real-life HST. As a matter of fact, since our "exact" model (3) is derived in symbolic mass, inertia, etc., parameter terms and our controller design procedure is likewise expressed in terms of those same symbolic terms, it is a simple matter to re-evaluate our controller expressions and our simulation results for any given numerical values of HST/solar array parameter terms. Accordingly, the following two sets of numerical parameter values for Fig. 2 were chosen for our simulation studies.

For both the symmetric and asymmetric solar array cases:

$$\begin{array}{lll} l_{01} = 2.5\,\mathrm{m}, & l_{02} = 2.5\,\mathrm{m}, & l_g = 1.5\,\mathrm{m} \\ l_1 = 4.8\,\mathrm{m}, & l_2 = 4.8\,\mathrm{m} & \\ M_0 = 10{,}500\,\mathrm{kg}, & J_0 = 10{,}500\,\mathrm{kg\text{-}m^2} & \\ M_1 = 180\,\mathrm{kg}, & J_1 = 180\,\mathrm{kg\text{-}m^2} & \\ M_2 = 180\,\mathrm{kg}, & J_2 = 180\,\mathrm{kg\text{-}m^2} & \end{array} \quad (26)$$

For the case of dynamically symmetric solar arrays:
At the 0.6-Hz flex mode

$$k_{11} = 5.5, \qquad k_{12} = 0.001$$
$$k_{21} = 5.5, \qquad k_{22} = 0.001 \tag{27}$$

At the 0.11-Hz flex mode

$$k_{11} = 0.18, \qquad k_{12} = 0.001$$
$$k_{21} = 0.18, \qquad k_{22} = 0.001 \tag{28}$$

For the case of dynamically *asymmetric* solar arrays:
At the 0.6-Hz flex mode

$$k_{11} = 6.5, \qquad k_{12} = 0.01$$
$$k_{21} = 5.5, \qquad k_{22} = 0.001 \tag{29}$$

At the 0.11-Hz flex mode

$$k_{11} = 0.3, \qquad k_{12} = 0.001$$
$$k_{21} = 0.18, \qquad k_{22} = 0.001 \tag{30}$$

The set of HST controller parameter values chosen for use with Eqs. (27–30) are as follows:
For the TI control mode

$$\zeta = 0.9, \qquad \omega_n = 1.0 \tag{31}$$

For the AD control mode

$$\zeta = 0.7, \qquad \omega_n = 1.0 \tag{32}$$

Results from Closed-Loop Simulation Exercises of HST Model (3)

The "exact" nonlinear model (3) associated with Fig. 2 was simulated and exercised in a series of runs on a digital computer using the two cases of plant parameter values shown in Eqs. (27–30). In that series of simulation exercises, the control term u in Eq. (3) was implemented first as the TI controller (16) and associated state observer and then as the AD controller (24) and its associated state observer using the corresponding controller parameter values shown in Eqs. (31) and (32). To demonstrate the ultimate performance capabilities of the TI and AD control modes, control actuator saturation effects were not simulated in these concept demonstration exercises. The simulated excitation of the solar array oscillations was accomplished by applying random, once-in-a-while, short-duration, high-intensity external torque pulses (simulated torque "impulses") to one or the other of the solar array arms shown in Fig. 2. The resulting angular motions $\phi(t)$, $\theta_1(t)$, $\theta_2(t)$ of the HST main-body and flapping solar arrays for both the TI control mode and the AD control mode and for both the symmetric and asymmetric solar array cases are shown in the series of time plots presented in Figs. 5–7. The time plots in Fig. 5 clearly show the TI controllers' ability to quickly adapt to and counteract the time-varying disturbance torques induced by the vibrating solar arrays and thereby effectively isolate the HST main body from those disturbances while maintaining a high quality of setpoint regulation $\phi(t) \approx 0$.

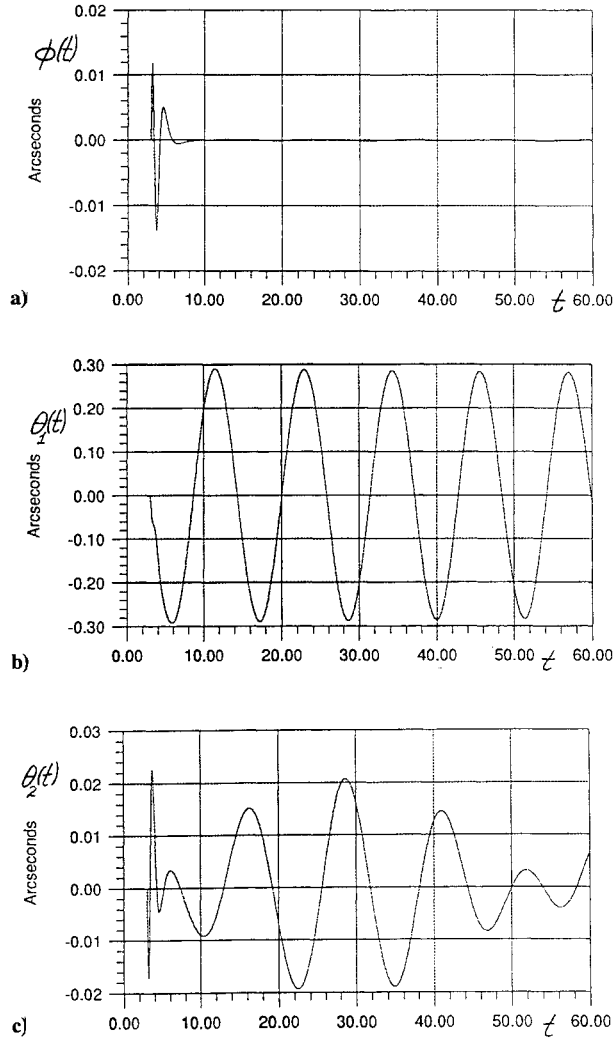

Fig. 5 Closed-loop responses for the TI control mode with dynamically asymmetric solar arrays (0.11 Hz, solar array oscillation triggered at t = 3.0 s).

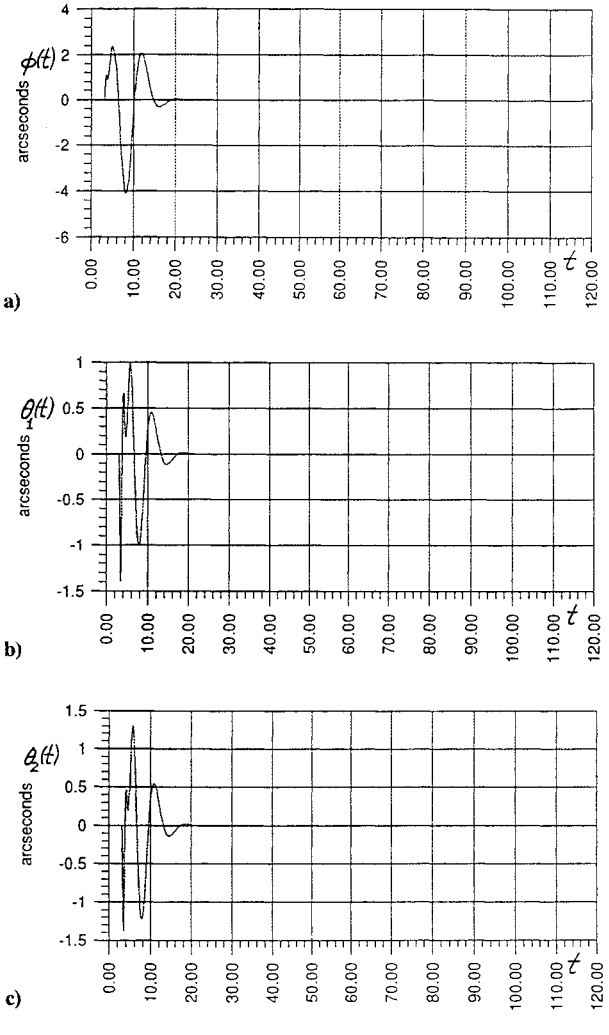

Fig. 6 Closed-loop responses for AD control mode with dynamically asymmetric solar arrays (0.6 Hz, solar array oscillation at t = 3.0 s).

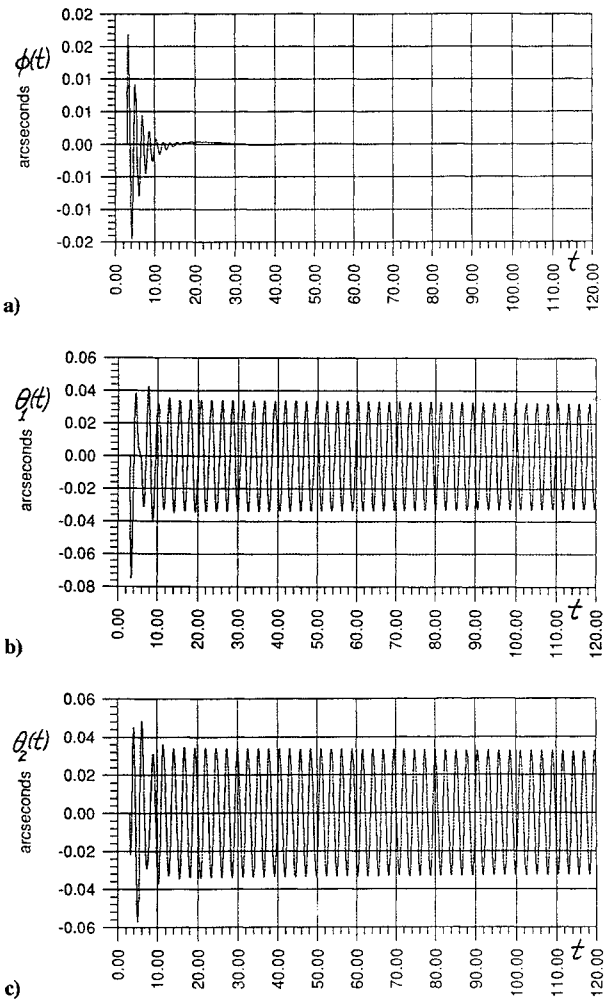

Fig. 7 Closed-loop responses for the AD control mode with dynamically symmetric solar arrays (0.6 Hz, solar array oscillation triggered at $t = 3.0$ s).

The closed-loop performances of $\phi(t)$, $\theta_1(t)$, $\theta_2(t)$ corresponding to the AD control mode are shown in Figs. 6 and 7. Those time plots demonstrate the ability of the AD controller to strategically maneuver the HST main-body motion $\phi(t)$ so as to actively augment the natural structural damping in the solar arrays and thereby hasten the rate at which $\theta_1(t) \rightarrow 0$, $\theta_2(t) \rightarrow 0$. It is interesting to note that, in the case of perfectly symmetric solar arrays (Fig. 7), the AD controller cannot distinguish which of the two solar arrays is causing the disturbing torques (i.e., a disturbance *un*observability condition arises in the composite plant/disturbance state observer used in the AD controller; see Appendix D of Ref. 1), and thus the AD controller cannot decide to which solar array it should direct the damping augmentation effort. Nevertheless, in that singular case, the AD controller automatically proceeds to maneuver the HST main body so that the two solar arrays are coerced into flapping in an equal-but-opposite (birdwing-like) manner, $\theta_1(t) \equiv -\theta_2(t)$, so that the corresponding net torque disturbance induced to the HST main body is thereby damped to zero, whereas $\theta_1(t) \rightarrow 0$ and $\theta_2(t) \rightarrow 0$ according to their natural damping characteristics.

When the two solar arrays are simulated as asymmetric, the disturbance unobservability condition cited in the previous paragraph does not occur, and the AD controller then succeeds in individually augmenting the natural damping of both $\theta_1(t) \rightarrow 0$ and $\theta_2(t) \rightarrow 0$ as evidenced in Fig. 6. It is remarked that the AD mode of control, as presently developed, exhibits a relatively small domain of (closed-loop) stability and tends to be rather sensitive to system parameter variations. These undesirable features, which appear to be a consequence of the nonlinear behavior of the terms $\boldsymbol{M}^{-1}(y)\boldsymbol{b}$ and $\boldsymbol{M}^{-1}(y)f(y, \dot{y})$ in the basic plant model (5), rather than a characteristic of the AD controller itself, constitute an important area for further research.

Computer-Animation Visualization of Simulated HST Closed-Loop Response Dynamics

The unique performance characteristics associated with the TI and AD control modes are dramatically evidenced by viewing a computer-generated animation of the controlled movements of the three-body HST model (main body and two attached "arms" representing the two solar arrays) as depicted in Fig. 2. For this purpose, the normal simulation data $\{\phi(t), \theta_1(t), \theta_2(t)\}$ were input into a specially prepared computer graphics program that repeatedly "draws" frames of Fig. 2 for a sequence of closely spaced discrete-time values t_k, $k = 0, 1, 2, 3, \ldots$. When that set of frames is displayed on the computer monitor in rapid sequence, one can "see" the three interconnected component bodies in Fig. 2, "moving" in planar-motion just as they would in reality. The intricate maneuvers of $\phi(t)$ one can thereby see being performed by the HST main body in the TI and AD control modes are rather impressive.

A VHS video tape of the aforementioned computer-generated animation sequence was prepared as part of this research effort.

Recommendations for Further Work

The recommendations for further work on this new HST control concept, along the lines presented here, are as follows:

1) Generalize the configuration model (Fig. 2) and the associated exact equations of motion to include arbitrary, three-axis, coupled angular motions for both the HST main body and the attached solar arrays. Include multiple modes of solar array oscillations.

2) Derive the three-axis TI and AD controller equations corresponding to the generalized three-axis model of HST. Generalize the AD controller equations to accommodate the nonlinear terms in the HST model.

3) Revise the TI and AD controller equations, as needed, for implementation in digital control format.[5]

4) Demonstrate the closed-loop performance of the three-axis HST model and associated three-axis TI/AD controllers by computer simulation exercises using actual HST controller actuator saturation levels and realistic values for masses, inertia, and other HST/solar array model parameters.

Summary and Conclusions

In this paper we have developed, and demonstrated by simulation exercises, a new dual-mode HST control concept for accommodating time-varying, persistent, uncertain torque disturbances (such as those due to flex-body "flapping" of the solar arrays) that act on the HST main body and degrade precision pointing of the HST. The new controller consists of two distinct control modes. In the TI control mode (envisioned as the primary mode of control), the HST control torques automatically synchronize with and adapt to the time-varying disturbance torques (in an equal-but-opposite sense) to effectively counteract and cancel the effects of those disturbance torques in real time. As a result, the HST main body is dynamically "isolated" from the disturbance torques, thereby permitting a high-quality precision pointing of the HST in the face of such disturbances. The system closed-loop performance using the TI control mode exhibits a high degree of robustness.

In the AD control mode (likely to be used only occasionally, when not in a pointing experiment) the HST's control torques are used to strategically maneuver the angular rotations of the HST main body in a rocking, back-and-forth manner so as to induce an active damping (damping augmentation) effect to the natural damping of the solar array flex-body oscillations and thereby hasten the damping-out of those flex-body oscillations. When the AD control mode is used, the closed-loop system has the undesired feature of a relatively small domain of stability and relatively high sensitivities to system parameter variations, apparently due to the nonlinear terms in the plant model. A redesign of the AD controller to accommodate those nonlinear terms should mitigate this feature.

The qualitative performance capabilities of the proposed new HST dual-mode controller concept have been determined by closed-loop computer simulation exercises. Those simulations are based

on the exact, nonlinear equations of motion for a simplified, planar-motion, three-body configuration model of the HST and its solar arrays using a generic set of mass, inertia, and other parameter values that are considered to be scalewise representative of the actual HST and its solar array disturbances. The closed-loop performance capabilities exhibited in our simulation studies of this simplified (single-axis) HST model are considered to be representative of the performance that can be achieved for the actual HST using a full three-axis (angular axes) controller designed by the same methodology employed here.

The new HST dual-mode pointing controller developed in this paper can be adapted to a variety of similar space-based "pointing projects" where flex-body oscillations of attached appendages (long booms, antennas, etc.) cause pointing "disturbances."

Acknowledgments

Research of the second author was supported by NASA/Marshall Space Flight Center, under Contract NAS8-38609, DO 49, with the University of Alabama in Huntsville. The authors acknowledge the invaluable help of Mitchell Hunt, Ph.D. graduate student, UAH ECE Department, who developed the HST computer animation program described herein.

References

[1]Addington, S. I., and Johnson, C. D., "A Dual-Mode Disturbance-Accommodating Controller for the Hubble Space Telescope," *Advances in Astronautical Sciences*, Vol. 81, 1993, p. 575.

[2]Stengel, R. F., *Stochastic Optimal Control; Theory and Applications*, Wiley, New York, 1986.

[3]Johnson, C. D., "Accommodation of Disturbances in Linear Regulator and Servomechanism Problems," *IEEE Transactions on Automatic Control*, Vol. 16, No. 6, 1971, p. 635.

[4]Johnson, C. D., "Theory of Disturbance-Accommodating Controllers," *Control and Dynamic Systems: Advances in Theory and Applications*, Vol. 12, 1976, pp. 387–489.

[5]Johnson, C. D., "A Discrete-Time, Disturbance-Accommodating Control Theory for Digital Control of Dynamical Systems," *Control and Dynamic Systems: Advances in Theory and Applications*, Vol. 18, 1982, pp. 223–315.

[6]Johnson, C. D., "Disturbance-Accommodating Control; An Overview," *Proceedings of the 1986 American Control Conference*, Seattle, WA, June 1986, pp. 526–536.

[7]Johnson, C. D., "Effective Techniques for the Identification and Accommodation of Disturbances," *Proceedings of the Third NASA/DOD Controls-Structures Interaction Conference* (San Diego, CA), NASA Conf. Pub. No. 3041, Jan.–Feb. 1989, p. 163.

[8]Kane, T. R., and Levinson, D., *Dynamics, Theory and Applications*, McGraw-Hill, New York, 1985.